Available online at www.sciencedirect.com
ScienceDirect
Journal of Solid State Chemistry 180 (2007) 1743–1749
JOURNAL OF SOLID STATE CHEMISTRY
www.elsevier.com/locate/jssc

Synthesis and photocatalytic activity for water-splitting reaction of nanocrystalline mesoporous titania prepared by hydrothermal method

Jaturong Jitputti[a], Sorapong Pavasupree[a,b], Yoshikazu Suzuki[a], Susumu Yoshikawa[a,*]

[a]*Institute of Advanced Energy, Kyoto University, Uji, Kyoto 611-0011, Japan*
[b]*Department of Materials and Metallurgical Engineering, Faculty of Engineering, Rajamangala University of Technology Thanyaburi, Klong 6, Pathumthani, 12110, Thailand*

Received 18 November 2006; received in revised form 9 February 2007; accepted 18 March 2007
Available online 23 March 2007

Abstract

Nanocrystalline mesoporous TiO_2 was synthesized by hydrothermal method using titanium butoxide as starting material. XRD, SEM, and TEM analyses revealed that the synthesized TiO_2 had anatase structure with crystalline size of about 8 nm. Moreover, the synthesized titania possessed a narrow pore size distribution with average pore diameter and high specific surface area of 215 m^2/g. The photocatalytic activity of synthesized TiO_2 was evaluated with photocatalytic H_2 production from water-splitting reaction. The photocatalytic activity of synthesized TiO_2 treated with appropriate calcination temperature was considerably higher than that of commercial TiO_2 (Ishihara ST-01). The utilization of mesoporous TiO_2 photocatalyst with high crystallinity of anatase phase promoted great H_2 production. Furthermore, the reaction temperature significantly influences the water-splitting reaction.

Keywords: TiO_2; Mesoporous; Hydrothermal; Water splitting; Photocatalysis

1. Introduction

The photocatalytic decomposition of water into H_2 and O_2 over semiconductor materials has attracted much attention since the first invention of photochemical water splitting over TiO_2 photoelectrode proposed by Fujishima and Honda [1]. Since hydrogen is recognized as an environmental friendly and a highly efficient fuel, the production of H_2 by direct water splitting attainable without polluted by-products is one of the potential alternatives to produce fuel for future energy supply [2]. The utilization of an oxide semiconductor photocatalyst for water splitting is a promising technique because the photocatalyst is in the solid phase, which is relatively inexpensive, safe for operation, and resistant to deactivation.

Among various oxide semiconductors, TiO_2 has been considerably investigated and reported as one of the most suitable materials in a wide range of technological applications including environmental pollutant cleanup and photocatalysis applications because of its photoreactivity, nontoxicity, long-term supply, and low price [3–5]. Several studies have reported that the surface properties of TiO_2 including grain size, crystallization, morphology, specific surface area, surface state, and porosity obviously influence the photocatalytic activity of TiO_2 [6–8]. Various synthesis methods, such as hydrothermal [8–13], sol–gel [14], and microemulsion (reverse micelles) [15], have been used to fabricateTiO_2 nanoparticles. Compared with the other methods, hydrothermal synthesis has more advantages [8,10,13]: (1) crystallization temperature for anatase phase is below 200 °C; (2) by adjusting the hydrothermal reaction condition, such as temperature, pressure, duration of process, reactant concentrations and pH value of solution, crystalline grain size, particle morphology, microstructures, phase composition and surface chemical properties; and (3) low-energy consumption and environmentally friendly process.

Recently, several papers have shown that TiO_2 photocatalyst has potential for photocatalytic water-splitting reaction [16–19]. Moreover, by doping metal co-catalysts,

*Corresponding author. Fax: +81 774 38 3508.
E-mail address: s-yoshi@iae.kyoto-u.ac.jp (S. Yoshikawa).

0022-4596/$ - see front matter © 2007 Elsevier Inc. All rights reserved.
doi:10.1016/j.jssc.2007.03.018

such as Pt, Au, Cu, and Ni, the photocatalytic activity could be enhanced [14,20–22]. In our previous work [14,23], we found that mesoporous titania photocatalyst synthesized via the surfactant-assisted templating sol–gel process showed high photocatalytic activity for H_2 production from water-splitting reaction.

In this study, hydrothermal method was reported as a potential method for mesoporous TiO_2 synthesis. The physical properties of the mesoporous TiO_2 were thoroughly studied in relation to its photocatalytic activity for H_2 production from water-splitting reaction. Furthermore, the dependence of the reaction temperature on the amount of the H_2 produced was also investigated.

2. Experimental

2.1. Photocatalyst synthesis

Nanocrystalline mesoporous TiO_2 photocatalyst was synthesized via hydrothermal method. In typical synthesis, 5.45 g of titanium butoxide (TIBU) was first introduced into acetylacetone (ACA) with the same mole. The mixed solution was then gently stirred in the Teflon-line stainless autoclave until intimate mixing. Afterward, 20 mL of ethanol followed by 20 mL of distilled water was slowly added into the reactor. The reactor was then kept 130 °C with stirring for 12 h. After that, it was naturally cooled down to room temperature. The product mixture was then washed by 2-propanol several times. It was dried in oven for overnight to obtain as-synthesized TiO_2. The as-synthesized TiO_2 was then calcined at 400–600 °C for 1 h to produce nanocrystalline mesoporous TiO_2.

2.2. Characterization

Simultaneous thermogravimetry and differential thermal analysis (TG–DTA; Shimazu DTG-50) was used to study the thermal decomposition behavior of the as-synthesized (dried) photocatalyst. The crystalline structure of samples was evaluated by X-ray diffractometer (XRD; RIGAKU RINT 2100). The microstructure of the prepared materials was analyzed by scanning electron microscopy (SEM; JEOL JSM-6500FE) and transmission electron microscopy (TEM; JEOL JEM-200CX). The nitrogen adsorption/desorption isotherms and BET specific surface area (S_{BET}) of the prepared TiO_2 were measured by using BEL Japan BELSORP-18 Plus equipment.

The average crystal sizes were estimated from the line broadening of X-ray diffraction reflections using the Sherrer formula [24] as follows:

$$L = \frac{k\lambda}{\beta \cos\theta}, \quad (1)$$

where L is the crystallite size, k the Sherrer constant (0.89 in this study), λ the wavelength of the X-ray radiation (0.15418 nm for Cu$K\alpha$), and β the full-width half-maximum (FWHM) in X-ray diffraction reflections measured at 2θ: baseline and FWHM of samples were determined by using JADE software (RIGAKU). The calculation is a simple estimation, and used for the comparison. Corrections for strain and equipment were not done.

2.3. Photocatalytic hydrogen production

Photocatalytic H_2 production reaction was carried out in a closed gas-circulation system (Fig. 1). TiO_2 photocatalyst (0.8 g) was suspended in aqueous methanol solution (800 mL distilled H_2O, 80 mL methanol) by means of magnetic stirrer within an inner irradiation-type reactor (1100 mL) made of Pyrex glass. A high-pressure Hg lamp (Ushio; UM-452, 450 W) was utilized as the light source. Prior to the reaction, the mixture was deaerated by purging with Ar gas repeatedly. To maintain the reaction temperature during the course of reaction, cooling water was circulated through a cylindrical Pyrex jacket located around the light source. The gaseous H_2 produced was periodically analyzed by an on-line gas chromatograph (Shimadzu GC-8A, Molecular sieve 5A, TCD, Ar carrier).

3. Results and discussion

3.1. Photocatalyst characterizations

The TG–DTA curves of the as-synthesized TiO_2 are shown in Fig. 2. From the DTA curve, it can be seen that an endothermic peak at below 100 °C is due to the desorption of water and alcohol, whereas the first exothermic peak at 246 °C, which is very sharp and narrow, and the second exothermic peak at 373 °C, which is weak and broad, are attributed to the thermal decomposition of the organic substance as the evidence of weight loss ended at 400 °C. Since the TG curve shows that weight loss ended at 400 °C and total weight loss until this temperature was 10.7 wt%, minimum calcination tempera-

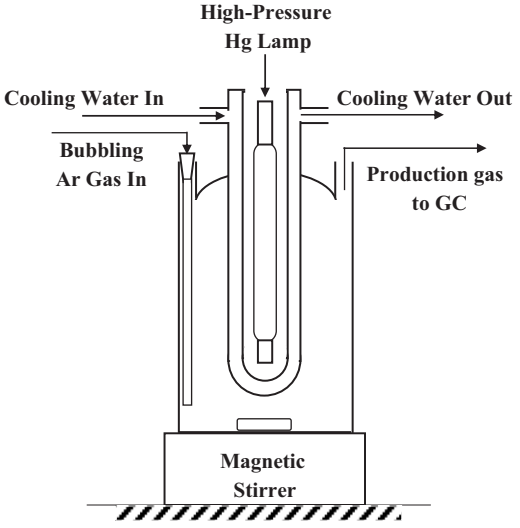

Fig. 1. Experimental apparatus.

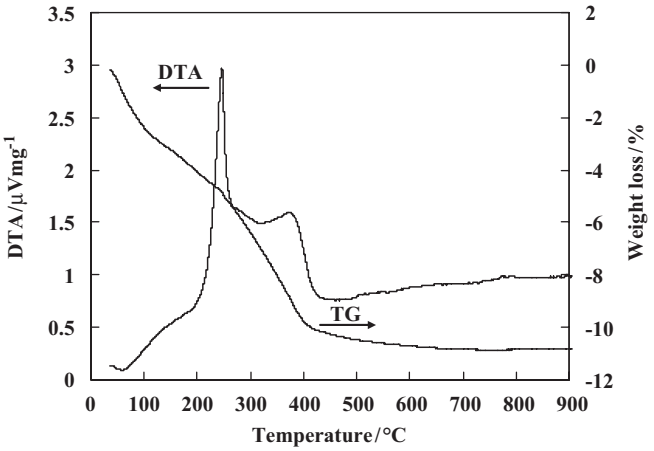

Fig. 2. TG–DTA curves of the as-synthesized TiO_2.

ture at this value, i.e., 400 °C, was sufficient for complete removal of the organic substance. After organic removal, all of the mesoporous TiO_2 samples turned from yellow (as-synthesized TiO_2) to white color. To examine the effects of synthesis variables for photocatalyst preparation, calcination temperature was increased from 400 to 600 °C at calcination time of 1 h.

Fig. 3 shows the XRD patterns of prepared TiO_2 samples in comparison with that of Ishihara ST-01 used as TiO_2 references. The phase identification and approximate crystallite size of the photocatalyst from XRD analysis are summarized in Table 1.

The XRD patterns of the samples calcined from 400 to 550 °C showed that the samples were composed of anatase phase. The dominant peaks at 2θ of about 25.2°, 37.9°, 47.8°, 53.8°, and 55°, which represent the indices of (101), (004), (200), (105), and (211) planes, respectively, are conformed to crystalline structure of anatase phase. However, the calcination temperature of 550 °C was determined as the highest limit for yielding well-crystallized pure anatase phase TiO_2 prepared by this synthetic system. While the sample calcined at 600 °C, partial phase transformation from anatase to rutile was observed, resulting in the combination of anatase and rutile phases. The occurrence of the dominant peaks at 2θ of about 27.4°, 36.1°, 41.2°, and 54.3° indicates the presence of rutile phase in the materials at this calcination temperature correspond to the indices of (1 1 0), (1 0 1), (1 1 1), and (2 1 1) planes, respectively. Furthermore, it is clearly seen that regardless of the phase present, increase in calcination temperature resulted in higher crystallinity, indicating the grain growth of TiO_2 crystallites as shown in Table 1. However, since the mesopores are not ordered in our samples, clear peaks cannot be detected by low-angle XRD measurement (see Supplementary data) from $2\theta = 0.4°$ to 1.5°, corresponding to 6–22 nm. However, some broad peaks and peak-tails can be detected and they may correspond to the intergranular mesopores.

The N_2 adsorption/desorption isotherms of the synthesized TiO_2 exhibited typical IUPAC type IV pattern with

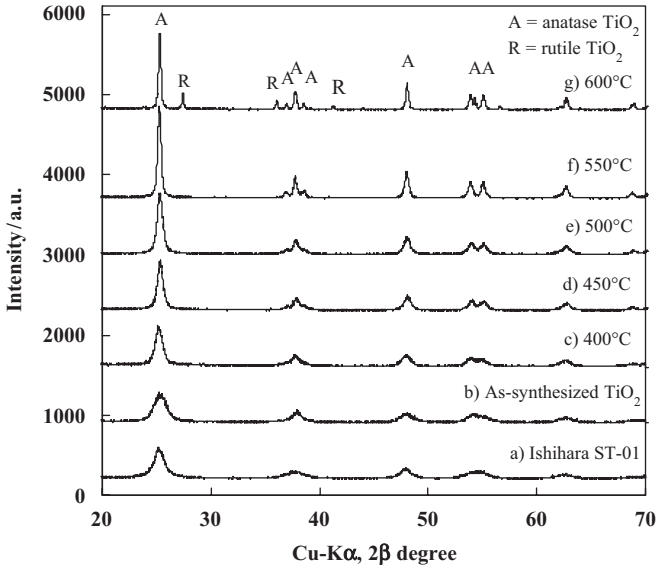

Fig. 3. XRD patterns of the mesoporous TiO_2 calcined at various temperatures. Note that Ishihara ST-01 is included for comparison.

the presence of hysteresis loop as exemplified in Fig. 4(a) for the sample calcined at 500 °C for 1 h, which provided the highest photocatalytic H_2 evolution activity (based on 0.8 g of TiO_2) as discussed later. The hysteresis loop is typically ascribed to the existence of mesopores in the sample. As illustrated in the inset in Fig. 4(a), the pore size distribution calculated by BJH method of samples obtained from this hydrothermal method is quite narrow, verifying good quality of the samples. In contrast, the isotherms of Ishihara ST-01 in Fig. 4(b) were completely different from that of the synthesized TiO_2. Owing to IUPAC classification, it was associated with type II sorption behavior, which is generally obtained with nonporous or macroporous (large pore diameter of >50 nm) materials.

The experimental results on BET surface area, mean pore diameter, and total pore volume of all synthesized materials are summarized in Table 1. As obviously seen, the surface area decreased from 122 to 29 m^2/g with increasing calcination temperature from 400 to 600 °C. The observed loss in surface area is attributable to increase in particle size associated with grain growth due to the crystallization of TiO_2 particle. Subsequently, this tendency caused an increase in mean pore diameter and a decrease in total pore volume of the bulk materials, as expected.

Fig. 5(a) and (b) shows SEM and TEM images of the mesoporous TiO_2 calcined at 500 °C for 1 h, respectively. SEM image in Fig. 5(a) indicates that the TiO_2 nanoparticles are reasonably uniform in size. The presence of mesopore could be partly observed by SEM analysis. In addition, TEM image in Fig. 5(b) demonstrates the formation of highly crystalline TiO_2 aggregates composed of three-dimensional disordered primary nanoparticles. The average size of the TiO_2 nanoparticles is approximately 14 nm, which is consistent with the crystallite size estimated from XRD analysis.

Table 1
Summary of XRD and N_2 adsorption–desorption analyses of the synthesized mesoporous TiO_2 and Ishihara ST-01

Material	Calcination temperature (°C)	Phase from XRD pattern	Crystalline size[a] (nm)		S_{BET} (m^2/g)	Mean pore diameter (nm)	Total pore volume (cm^3/g)
			Anatase/101	Rutile/110			
Synthesized TiO_2[b]	As-synthesized	Anatase	8.2	—	215	9.1	0.520
	400	Anatase	11.5	—	122	9.9	0.406
	450	Anatase	14.3	—	109	9.7	0.365
	500	Anatase	14.7	—	101	9.9	0.322
	550	Anatase	21.8	—	37	18.4	0.155
	600	Anatase + Rutile	31.6	42.3	29	20.2	0.129
Ishihara ST-01[c]	—	Anatase	10.4	—	300	—	—

[a]Approximation by using Sherrer formula.
[b]N_2 adsorption–desorption isotherm corresponds to IUPAC type IV pattern.
[c]N_2 adsorption–desorption isotherm corresponds to IUPAC type II pattern.

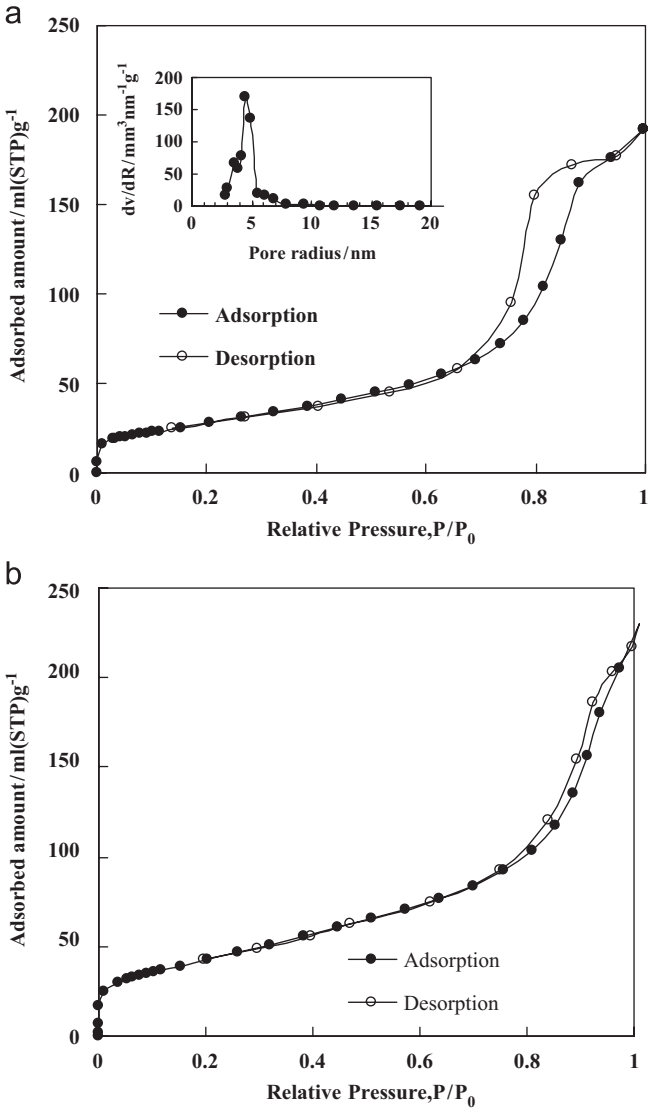

Fig. 4. (a) N_2 adsorption–desorption isotherm and pore size distribution (inset) of the nanocrystalline mesoporous TiO_2 calcined at 500 °C for 1 h. (b) N_2 adsorption–desorption isotherm of Ishihara ST-01.

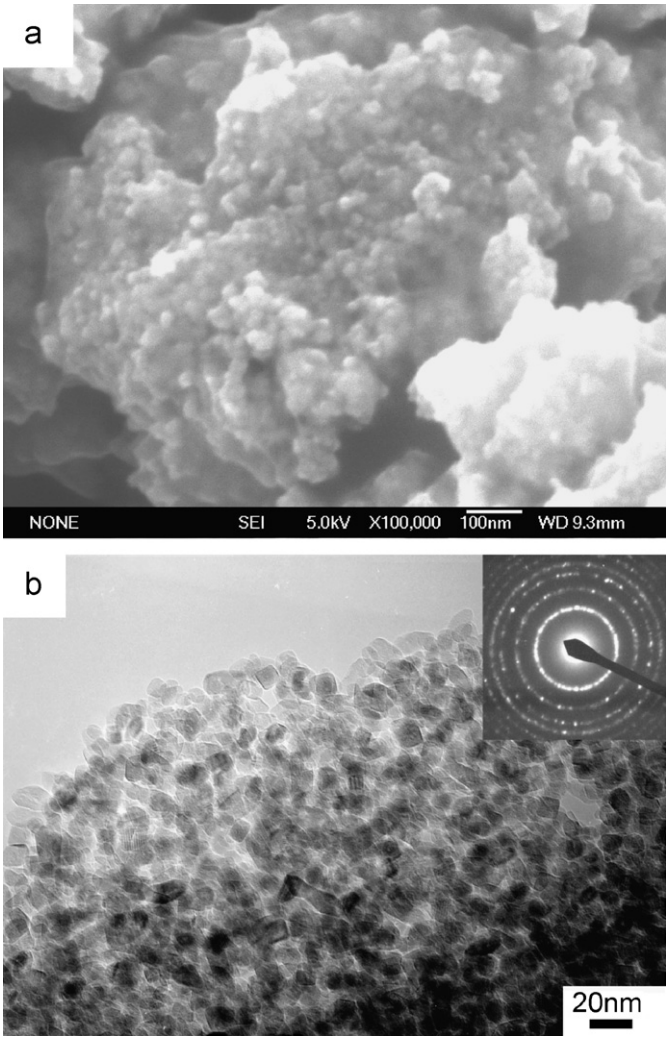

Fig. 5. SEM (a) and TEM (b) images of the mesoporous TiO_2 calcined at 500 °C for 1 h.

3.2. Photocatalytic H_2 production

The photocatalytic H_2 production activity of mesoporous TiO_2 calcined at various temperatures compared with commercial TiO_2 (Ishihara ST-01) was measured under UV light irradiation. No appreciable H_2 production was detected in the absence of either UV light irradiation or TiO_2 photocatalyst. However, in the presence of both, detectable H_2 was observed. This therefore confirmed that gaseous H_2 produced was in fact generated from photocatalyzed water splitting over TiO_2 photocatalyst under UV light irradiation.

Fig. 6 demonstrates the time course of the photocatalytic H_2 production from water-splitting reaction over the mesoporous TiO_2 calcined at various temperatures and Ishihara ST-01. It was found that, based on the amount of photocatalyst (0.8 g), the photocatalytic H_2 evolution activity of the mesoporous TiO_2 calcined at 400–550 °C was higher than that of Ishihara ST-01, whereas the mesoporous TiO_2 calcined at 600 °C showed lower photocatalytic H_2 evolution activity. The loss in photocatalytic activity of mesoporous TiO_2 calcined at 600 °C was attributed to the low surface area and the presence of rutile phase of sample calcined at this temperature and this consequently resulted in low photocatalytic activity [23]. It has been reported that TiO_2 anatase phase shows a higher photocatalytic activity than TiO_2 rutile due to its low recombination rate of photogenerated electrons and holes [8]. As shown in Fig. 3, the phase transformation of the mesoporous TiO_2 from anatase to rutile phase occurred at this calcination temperature (600 °C).

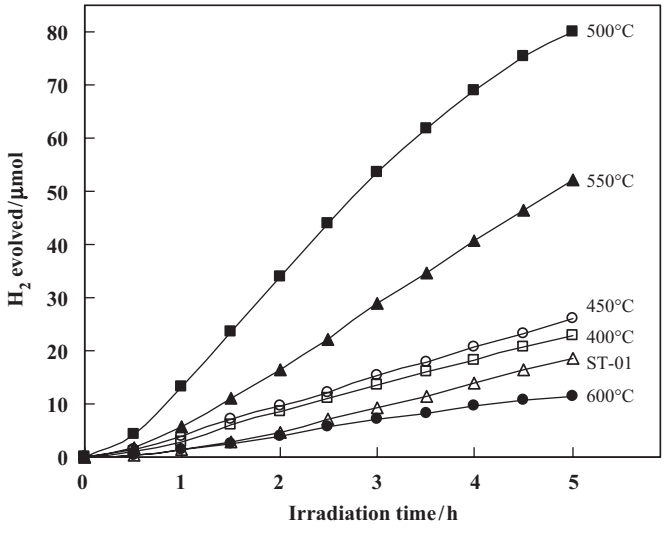

Fig. 6. Photocatalytic H_2 production from water-splitting reaction over the mesoporous TiO_2 calcined at various temperatures and commercial TiO_2 (Ishihara ST-01): TiO_2 ST-01 (△), mesoporous TiO_2 calcined at 400 °C (□), 450 °C (○), 500 °C (■), 550 °C (▲), and 600 °C (●); 0.8 g TiO_2 photocatalyst, aqueous methanol solution (80 mL CH_3OH, 800 mL H_2O), irradiation time 5 h. Note that the Ishihara ST-01 TiO_2 powder was used as received.

The amount of gaseous H_2 produced from Ishihara ST-01 after 5 h UV light irradiation at identical reaction conditions is 19 μmol, while the highest photocatalytic H_2 production from the mesoporous TiO_2 treated with optimum calcination temperature at 500 °C was observed to be 80 μmol. In comparison with the photocatalytic activity, the mesoporous TiO_2 treated under suitable condition provided much higher H_2 production than commercial TiO_2 (Ishihara ST-01). Despite large surface area about 300 m^2/g of Ishihara ST-01, imperfect crystallization accompanied with fairly small crystallite size (Table 1) is considered to favorably increase the probability of mutual e^-/h^+ recombination at both surface and bulk traps. In contrary, the use of the nanocrystalline mesoporous TiO_2 with high crystallinity could decrease the number of lattice defects and then facilitate the electron transport for reacting with water molecule adsorbed at TiO_2 surface along the mesopore structure leading to much better photocatalytic performance as mention in our previous work [23].

The dependence of the calcination temperature on the amount of H_2 production per S_{BET} of photocatalyst is illustrated in Fig. 7. The results indicated that the photocatalytic H_2 production activity considerably depended on calcination temperature. The investigated calcination temperatures were 400, 450, 500, 550, and 600 °C at the calcination time of 1 h. It was found that all of mesoporous TiO_2 prepared in this study shows photocatalytic H_2 production activity higher than that of the commercial one (ST-01). Among these calcination temperatures, the maximum H_2 production per S_{BET} was observed at calcination temperature of 550 °C. The explanations can be assorted into two parts, namely, prior to and behind the highest values. Firstly, in spite of larger surface area of the materials calcined at lower calcination temperature prior to the peak (1.41 μmol/m^2), the higher

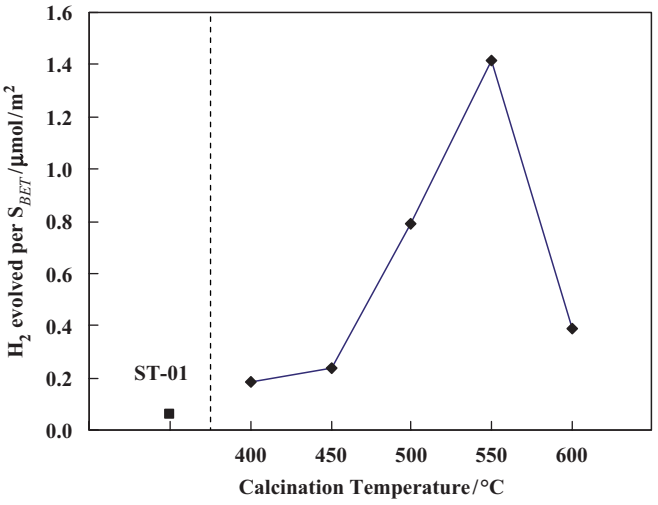

Fig. 7. Dependence of the calcination temperature on the amount of H_2 production per S_{BET} of TiO_2; 0.8 g photocatalyst, aqueous methanol solution (80 mL CH_3OH, 800 mL H_2O), irradiation time 5 h. Note that the Ishihara ST-01 TiO_2 powder was used as received.

photocatalytic activity at higher calcination temperature implied that crystallinity plays a more significant role in the photocatalytic H_2 production activity. It was mentioned that higher crystallinity has been evaluated to drastically affect the higher photocatalytic activity of TiO_2 materials [7,25]. Therefore, it could be inferred that although surface area of the mesoporous TiO_2 calcined at 550° C was smaller than that of 400, 450, and 500 °C, better crystallization of anatase phase from inspection of XRD patterns is intensely considered as a major advantage. In addition, the amorphous phase contained to some extent in the mesoporous TiO_2 calcined at low calcination temperature has been reported to have a negative effect on the photocatalytic activity for H_2 production, since amorphous phase, which usually comprises numerous defects, i.e., impurities, dangling bonds, and microvoids, can behave as recombination centers for the photoinduced e^-/h^+ pairs resulting in decreasing the photocatalytic activity [26].

It can be clearly seen that smaller surface area was achieved, whereas higher crystallinity was conversely observed with increasing calcination temperature. By taking this into account, the expected increment of the photocatalytic activity owing to the increase in crystallinity (less number of lattice defects) may exceed the expected decrement of the photocatalytic activity owing to the decrease in the surface area. Therefore, the balance of these two conflicting factors that affect photocatalytic activity is very important for photocatalytic H_2 production.

In the second part, when the synthesized TiO_2 was calcined at temperature higher than 550 °C, the amount of H_2 production per S_{BET} decreased with increasing calcination temperature, although higher crystallinity was attained. Generally, increment of calcination temperature brought about a loss of mesopores to a great extent, and consequently, lower surface area. The decrease in surface area resulted in decreasing the number of active reaction sites and subsequently less accessibility of the reactant, water molecule, to adsorb onto the photocatalyst surface, react with the photogenerated electron, and produce the gaseous H_2. Hence, it could be concluded that the surface area of the synthesized TiO_2 materials predominantly governed the photocatalytic H_2 production activity in the second range.

In case of mesoporous TiO_2 calcined at 600 °C (0.39 μmol/m^2), however, the photocatalytic H_2 production activity (H_2 production per S_{BET}) was found to be higher than that of samples calcined at 400 °C (0.19 μmol/m^2) and 450 °C (0.24 μmol/m^2), and ST-01 (0.06 mmol/m^2) even though the S_{BET} of sample calcined at 600 °C was much lower than that of samples calcined at 400 and 450 °C, and ST-01 (Table 1). This therefore supported that the crystallinity of TiO_2 anatase phase plays a more important role in the photocatalytic H_2 production activity.

The dependence of reaction temperature on the amount of H_2 was also investigated and is shown in Fig. 8. By varying the cooling water temperature, the amount of H_2 produced increased about 8 times when the cooling water temperature increased from 25 to 30 °C. It can be concluded that the reaction temperature also plays more important role for water-splitting reaction from aqueous methanol solution.

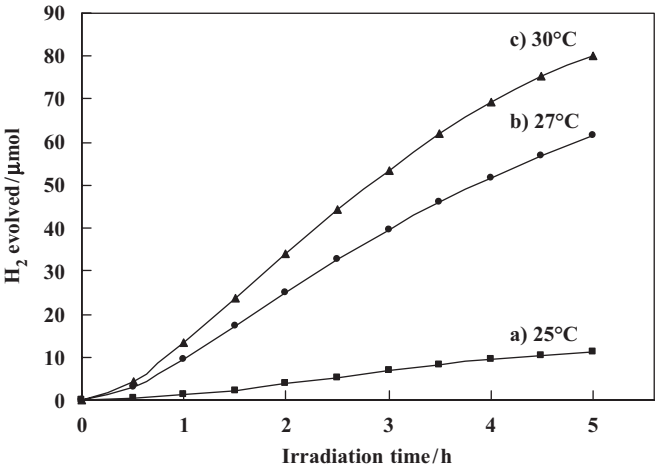

Fig. 8. Dependence of reaction temperature on the amount of H_2 production: (a) 25 °C, (b) 27 °C, and (c) 30 °C; 0.8 g mesoporous TiO_2 calcined at 500 °C for 1 h, aqueous methanol solution (80 mL CH_3OH, 800 mL H_2O), irradiation time 5 h.

4. Conclusion

High surface area nanocrystalline mesoporous TiO_2 with high photocatalytic activity for H_2 production can be simply synthesized by hydrothermal method. The utilization of the synthesized mesoporous TiO_2 calcined at all temperatures (400–600 °C) showed better photocatalytic H_2 production than that of commercial TiO_2 (Ishihara ST-01), especially the synthesized TiO_2 calcined at optimum temperature of 550 °C for 1 h, which promoted much considerably higher H_2 production rate (1.41 μmol/m^2). Furthermore, it should be noted that, for this synthetic system, the crystallinity and crystal structure of the synthesized TiO_2 chiefly govern the photocatalytic H_2 production activity rather than the surface area. Therefore, by taking this into account, the balance of these two conflicting intrinsic properties, i.e., crystallinity and surface area, is very important for photocatalytic H_2 production. In addition, the presence of rutile phase in synthesized TiO_2 also resulted in low photocatalytic activity. Hence, to obtain high photocatalytic H_2 production activity, it is crucial to control the thermal treatment conditions leading to high crystallinity of anatase phase without the formation of rutile phase. The order of photocatalytic H_2 production (based on weight of photocatalyst) is mesoporous TiO_2 calcined at 500 °C > 550 °C > 450 °C > 400 °C > ST-01 > 600 °C. In case of the photocatalytic activity based on the amount of H_2 produced per active reaction site (μmol/m^2), the photoactivity can be shown from highest to lowest as follows: 550 °C > 500 °C > 600 °C > 450 °C > 400 °C > ST-01. Moreover, the reaction temperature significantly influences the amount of H_2 produced.

Acknowledgments

This work was financially supported by the Grant-in-Aid for Scientific Research from the Ministry of Education, Science, Sports, and Culture, Japan, under the 21COE program. Gratefulness is forwarded to Prof. S. Isoda and Prof. H. Kurata at the Institute for Chemical Research, Kyoto University, for their support of TEM apparatus. The authors show great appreciation to S. Katao and A. Kitiyanan, Graduate School of Materials Science, NARA Institute of Science and Technology, for his XRD measurement assistance. T. Sreethawong is acknowledged for his help on setup of the apparatus.

Appendix A. Supplementary data

Supplementary data associated with this article can be found in the online version at doi:10.1016/j.jssc.2007.03.018.

References

[1] A. Fujishima, K. Honda, Nature 238 (1972) 37–38.
[2] K. Shimizu, S. Itoh, T. Hatamachi, T. Kodama, M. Sato, K. Toda, Chem. Mater. 17 (2005) 5161–5166.
[3] W. Ho, J.C. Yu, J. Mol. Catal. A: Chem. 247 (2006) 268–274.
[4] A. Fujishima, T.N. Rao, D.A. Tryk, J. Photochem. Photobiol. C: Photochem. Rev. 1 (2000) 1–21.
[5] D.F. Ollis, H. Al-Ekabi, Photocatalytic Purification and Treatment of Water and Air, Elsevier Science Publishers, New York, 1993.
[6] V. Subramanian, E.E. Wolf, P.V. Kamat, J. Am. Chem. Soc. 126 (2004) 4943–4950.
[7] B. Ohtani, Y. Ogawa, S. Nishimoto, J. Phys. Chem. B 101 (1997) 3746–3752.
[8] J. Yu, G. Wang, B. Cheng, M. Zhou, Appl. Catal. B: Environ. 69 (2007) 171–180.
[9] H. Kominamia, J. Kato, S. Murakami, Y. Kera, M. Inoue, T. Inui, B. Ohtani, J. Mol. Catal. A Chem. 144 (1999) 165–171.
[10] M. Wu, J. Long, A. Huang, Y. Luo, Langmuir 15 (1999) 8822–8825.
[11] Y. Yue, Z. Gao, Chem. Commun. (2000) 1755–1756.
[12] L. Wu, J.C. Yu, X. Wang, L. Zhang, J. Yu, J. Solid State Chem. 178 (2005) 321–328.
[13] J. Yu, Y. Su, B. Cheng, M. Zhou, J. Mol. Catal. A: Chem. 258 (2006) 104–112.
[14] T. Sreethawong, Y. Suzuki, S. Yoshikawa, Int. J. Hydrogen Energy 30 (2005) 1053–1062.
[15] E. Stathatos, P. Lianos, F.D. Monte, D. Levy, D. Tsiourvas, Langmuir 13 (1997) 4295–4300.
[16] K. Sayama, H. Arakawa, J. Photochem. Photobiol. A: Chem. 77 (1994) 243–247.
[17] R. Abe, K. Sayama, K. Domen, H. Arakawa, Chem. Phys. Lett. 344 (2001) 339–344.
[18] N. Wu, M. Lee, Z. Pon, J. Hsu, J. Photochem. Photobiol. A: Chem. 163 (2004) 277–280.
[19] A.A. Nada, M.H. Barakat, H.A. Hamed, N.R. Rohamed, T.N. Veziroglu, Int. J. Hydrogen Energy 30 (2005) 687–691.
[20] D. Jing, Y. Zhang, L. Guo, Chem. Phys. Lett. 415 (2005) 74–78.
[21] N.L. Wu, M.H. Lee, Int. J. Hydrogen Energy 29 (2004) 1601–1605.
[22] G.R. Bamwenda, S. Tsubota, T. Nakamura, M. Haruta, J. Photochem. Photobiol. A: Chem. 89 (1995) 177–189.
[23] T. Sreethawong, Y. Suzuki, S. Yoshikawa, Catal. Commun. 6 (2005) 119–124.
[24] B.D. Cullity, Elements of X-ray Diffraction, Addison-Wesley Pub. Co., Reading, MA, 1978.
[25] V.F. Stone Jr., R.J. Davis, Chem. Mater. 10 (1998) 1468–1474.
[26] C.N.R. Rao, K.J. Rao, Phase Transitions in Solids: An Approach to the Study of the Chemistry and Physics of Solids, McGraw-Hill, New York, London, 1978.